CMOS Realizations of the Operational Mirrored Amplifier

A. Soltan
Fayoum University,
Fayoum, Egypt

A. M. Soliman
Cairo University,
Cairo, Egypt
asoliman@ieee.org

Abstract: *Four designs of a high performance CMOS Operational Mirrored Amplifier (OMA) are presented. The proposed circuits are useful for implementing current – mode analog CMOS integrated circuits. The circuits are developed by using differential pair and the Floating Current Source (FCS) blocks. A low power class AB circuits are implemented in 0.25μm CMOS technology and their different characteristics are simulated. Design examples of realizing inverting and non-inverting current amplifier, Sallen – Key bandpass filter, voltage amplifier and voltage-to-current converter based on the proposed OMA realizations are given. Simulation results of the proposed circuits are included.*

Key words: *Operational mirrored amplifier, floating current source, bandpass, highpass, lowpass, dynamic biasing, current mode circuits, voltage-to-current converter, simulated inductor.*

1. Introduction

Analog circuit design using the current mode approach has recently gained considerable attention. This stems from its inherent advantages of wide bandwidth, high slew rate, low power consumption and simple circuitry [1].

Operational amplifier (OA) is a unique in the sense that the transfer functions are not dependant on the internal parameters of the realization [2]. OA is divided into four types; operational inverting amplifier (OIA) where both the input and output ports are connected to supply and ground, operational voltage amplifier (OVA) where only the output port is grounded and the input is floating, operational current amplifier (OCA) where the input port is grounded and the output ports are floating and the operational floating amplifier (OFA) where the input and output ports are floating. The main advantage of the OFA is that its high degree of isolation between input and output ports and the supply or ground terminals, and it can provide a high gain value.

The operational mirrored amplifier (OMA) is a general purpose current mode building block and basically a high gain transconductance scheme with identical output currents, which is the main difference between the OMA and the OFA [3-5].

OFA comprises a nullator at one port and a norator at the other port as illustrated in Fig. 1(a). According to the definition of the OFA, an ideal OFA is symbolically shown in Fig. 1(b). OFA exhibits these terminal characteristics: $I_+=I_-=0$, $V_+=V_-$ and $I_{o1}=-I_{o2}$. Similarly, the symbolic representation of the OMA is shown in Fig. 1(d). The pathological element representation of the OMA is shown in Fig. 1(c). It includes a nullator representing the input port and a current mirror representing the output port of the OMA [4]. The terminal characteristics of the OMA are: $I_+=I_-=0$, $V_+=V_-$ and $I_{o1}=I_{o2}$. The output of the OMA can be expressed by equation (1) where G_m is the open loop transconductance gain of the OMA. When a negative feedback is applied, the voltages at the two input ports are forced to be equal as expressed by equation (2).

$$I_{o1} = I_{o2} = G_m (V_+ - V_-) \quad (1)$$

$$V_+ = V_- \quad \text{as } Gm \longrightarrow \infty. \quad (2)$$

As the finite open loop gain G_m decreases, the difference between the two voltage increases. Therefore, the open loop transconductance gain is required to be as large as possible in order to improve the performance.

OMA realization was first presented in [5], then the full circuit was presented in [4]. In the proposed paper, the realization presented in [5] is modified to achieve better performance at low voltage.

The paper is organized as follow: Section 2 describes the CMOS realizations of the proposed OMA circuits. In section 3 the simulation results of the proposed realizations are presented. Finally, section 4 describes some applications of the proposed OMA circuit.

For all circuits examined in this paper, the supply voltages are ±1.5V. PSPICE simulations are carried out with model parameters of 0.25 μm level 3 CMOS process provided by MOSIS.

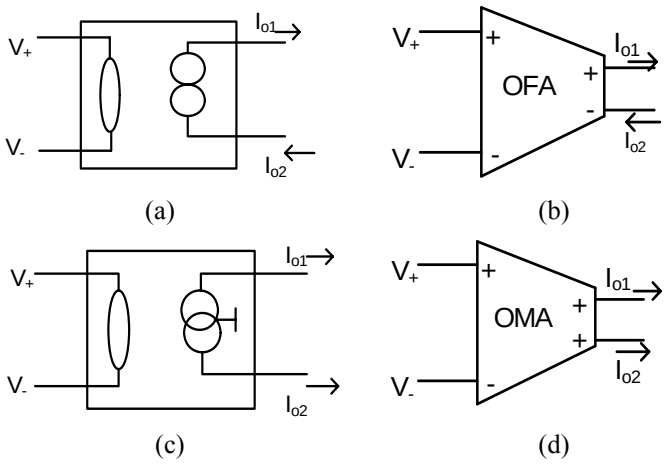

Fig. 1. (a) Nullor representation of the OFA; (b) Symbol of the OFA; (c) Pathological element representation of the OMA; (d) Symbol of the OMA.

2. New CMOS Realizations for the OMA

In this section four new CMOS realizations for the OMA are proposed and their circuit descriptions.

2.1. The CMOS Realization of Modified OMA

The block diagram of the OMA is that of a transconductance amplifier as shown in Fig. 2(a). Consequently, the core of the proposed OMA is simple CMOS transconductance amplifier. Fig. 2(b) depicts the realization of the proposed OMA where the transconductance amplifier is formed by a differential input stage M8 – M16 and a current output stage M17 - M28 with current source capability.

The requirement of large transconductance gain can't be achieved by a such configuration which is known to have a wide differential input range. A second differential stage is therefore added to increase the overall gain of the circuit to reduce the linear input voltage range. The differential input stage formed by transistors M1- M7 drives the transconductance stage by means of two level shifters M29 – M32 in order to provide proper level shifting and symmetrical operation mode. The transconductance of this configuration is given by

$$G_m = g_{m1}\left[r_{d2} // r_{d4} r_{d6} g_{m4}\right] g_{m9}\left[r_{d12} // r_{d14} r_{d16} g_{m14}\right] g_{m23} \quad (3)$$

Since in most applications the OMA is used in closed loop configuration, appropriate compensation is used to provide circuit stability. A compensating capacitor is connected between the two obvious high impedance nodes of the circuit. A third node, although of lower impedance, reduces the phase margin near unity gain frequency making the use of a second capacitor is a must.

By observing the proposed configuration shown in Fig.2 (b), the main difference between this configuration and that proposed in [5] is the load of the differential input stage. The circuit proposed in [5] was designed using cascode current source while the circuit proposed here is designed using low voltage current source [6-8], because the cascode configuration can't work at low voltage mode.

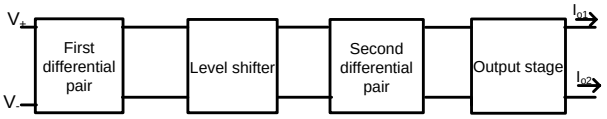

(a)

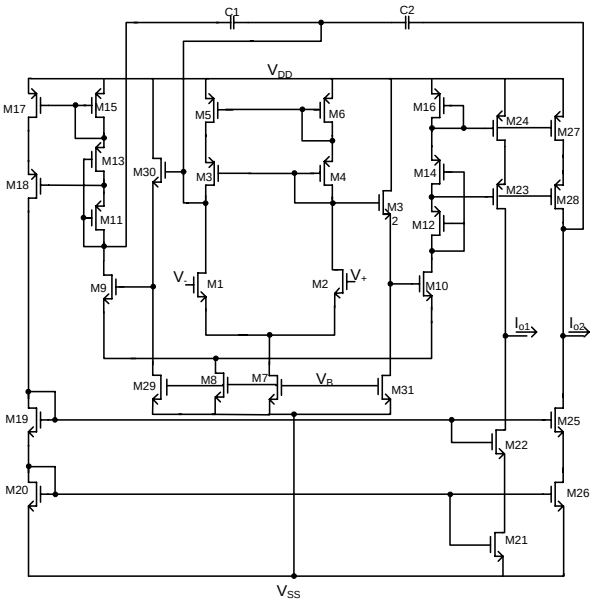

(b)

Fig. 2. (a) Block diagram of the modified OMA circuit; (b) The CMOS realization of the modified OMA circuit.

2.2. Wide Range OMA

To surpass the problem of low levels of the linear input voltage range of the modified OMA, a dynamic biasing technique has been applied to the first differential pair as shown in the block diagram of Fig. 3(a). The CMOS realization of the wide range OMA is shown in Fig.3 (b). The non-linearity of the differential pair is a result of the constant current drive. So, instead of biasing the differential pair with constant currents, a negative feedback stabilization circuit is required for the source nodes of the differential pair. This is achieved by means of

amplifier stage. This feedback circuit forces the common node to track the input common mode voltage. The transconductance of the OMA after feedback is given by:

$$G_m = g_{m1}\left[1-\frac{g_{m2}}{g_{m33}}\right]\left[r_{d2}//r_{d4}r_{d6}g_{m4}\right]g_{m9}\left[r_{d12}//r_{d14}r_{d16}g_{m14}\right]g_{m23} \quad (4)$$

Table 1. Transistor aspect ratio for the modified OMA circuit.

The transistor	Aspect ratio(W/L)
M1,M2	50/15
M3, M4	75/0.5
M5, M6	125/0.5
M7	60/10
M8 - M10	100/10
M11,M12	100/0.5
M13, M15,M17,M18	20/0.5
M14,M16,M19 – M28	20/5
M29 – M32	40/40

As shown in the CMOS realization of Fig. 3(b), the input stage is formed by a differential pair M1 – M7. This drives another differential pair stage M8 – M16 by means of two level shifters M17 – M20 to provide proper level shifting. The dynamic biasing circuit M33 – M37 is applied to the first differential pair in the input stage, to increase the input voltage range. Due to the use of feedback with the first differential pair the gain of the circuit is reduced. The second differential pair drives a current output stage M21 – M32 to provide the required output currents. The compensating capacitors C1 and C2 are connected between the high gain nodes of the OMA circuit to keep the circuit stability in feedback configuration.

2.3. High Gain OMA

To achieve high DC gain and large bandwidth, Floating Current Source (FCS) is used as an input stage for the OMA. FCS is very essential in analog signal processing circuits, because it gives high gain with large bandwidth [9, 10]. FCS also has the advantage that its inputs and outputs are isolated from the ground and the supply voltage nodes. So it can be used as an input stage for the OMA as shown in the block diagram of Fig. 4(a).

The input stage of the OMA circuit is formed by the FCS M1 – M7 which can be viewed as two differential pairs connected in parallel as shown in the CMOS realization in Fig. 4(b). This FCS drives a differential pair M12 – M20 loaded with a low voltage current mirror to operate at low voltage mode.

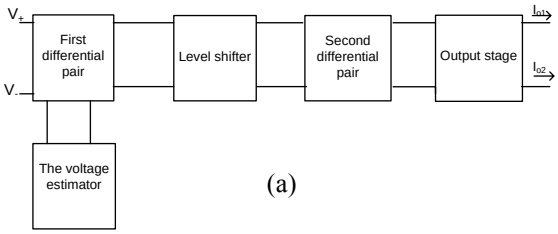

(a)

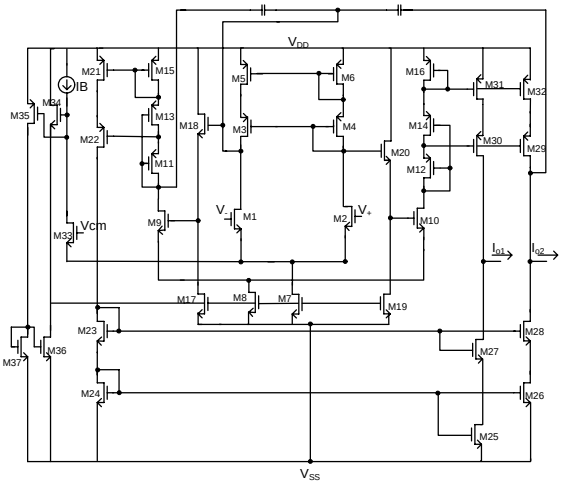

(b)

Fig. 3. (a) The block diagram of the wide range OMA circuit; (b) The CMOS realization of the wide range OMA circuit.

Table 2. Transistor aspect ratio for the wide range OMA circuit

Transistor	Aspect ratio (W/L)
M1,M2	50/20
M3,M4	75/0.5
M5,M6	125/0.5
M7	60/20
M8 – M10	100/5
M11,M12	100/0.5
M13,M15,M21,M22	20/0.5
M14,M16,M23 – M32	20/5
M17 – M20	20/20
M33	3.5/0.5
M34,M36	1.5/0.5
M35	7/0.5
M37	1/5

The differential pair is also biased using the dynamic biasing circuit M9 – M11 to increase its input voltage range and decrease the non-linearity region of operation for the differential pair. Finally, the

differential pair drives a current output stage M21 – M32 to drive the required output current. For this realization the transconductance is given by

$$G_m = \left(g_{m1}+g_{m3}\right)\left(r_{d2}//r_{d4}\right)g_{m13}\left[1-\frac{g_{m14}}{g_{m7}}\right]\left[r_{d15}//r_{d17}r_{d19}g_{m17}\right]g_{m29} \quad (5)$$

This circuit uses the FCS in the input stage instead of the differential pair to increase the overall gain of the circuit and also to increase the circuit bandwidth.

2.4. FCS – Based OMA

Another way to implement the OMA using the FCS is proposed here. The idea behind this approach is based on that the input and output ports of the FCS are isolated from the ground and the supply voltage. So it can be used as a building block for the OMA as shown in the block diagram in Fig. 5 (a).

As shown in the CMOS realization of Fig. 5(b), the input stage is represented by the FCS M1-M6, which drives another FCS M8 – M12. The second FCS drives a current output stage M13 –M21 to drive the required output currents.

The transconductance is given by

$$G_m = \left(g_{m1}+g_{m3}\right)\left(r_{d2}//r_{d4}\right)\left(g_{m9}+g_{m10}\right)\left(r_{d11}//r_{d12}\right)g_{m20} \quad (6)$$

In the sense that, the FCS gives high gain with large bandwidth, the proposed circuit gives the higher gain with larger bandwidth than the other realizations presented before as will be shown later in the simulations results.

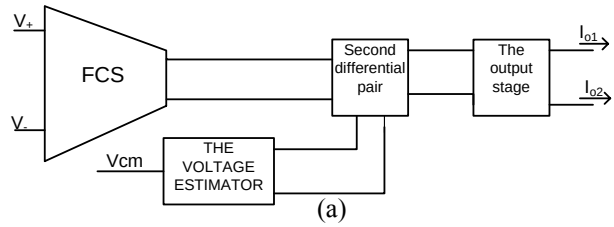

(a)

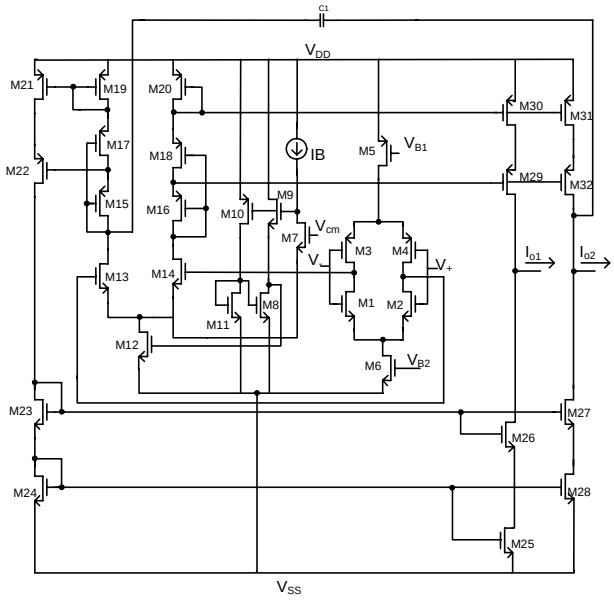

(b)

Fig. 4. (a) The block diagram of the High gain OMA; (b) The CMOS realization of the high gain OMA circuit.

Table 3. Transistor aspect ratio for the high gain OMA circuit

Transistor	Aspect ratio (W/L)
M1,M3,M5,M6	145/4.25
M2,M4	15/4.25
M7	3.5/0.5
M8,M9	1.5/0.5
M10	7/0.5
M11	1/5
M12 – M14	100/10
M15,M16	100/0.5
M17,M19,M21,M22	20/0.5
M18,M20,M23 – M32	20/5

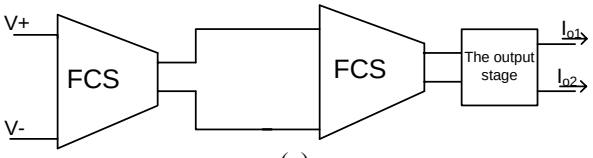

(a)

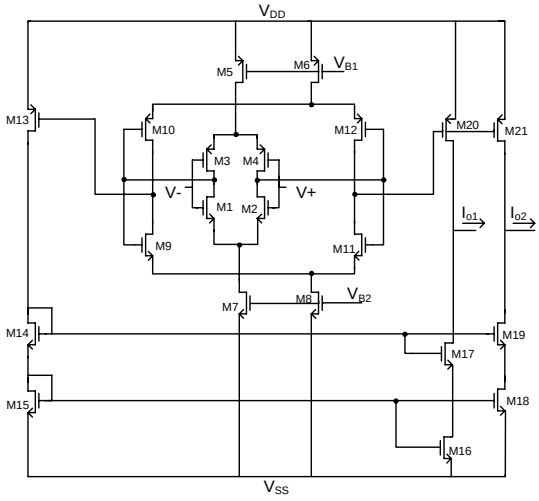

(b)

Fig. 5. (a) The block diagram of the FCS – Based OMA circuit; (b) The CMOS realization of the FCS – Based OMA circuit.

Table 4. The transistor aspect ratio for the FCS – Based OMA circuit

Transistor	Aspect ratio
M1 - M12	50/4.25
M13	300/0.5
M14 - M19	20/5
M20,M21	16/8

3. Simulation Results

To verify the performance of the proposed OMA configurations, a series of simulations using PSPICE were performed using transistor aspect ratios tabulated in tables (1 – 4), the supply voltages are ±1.5V, the bias voltage VB for the modified OMA is -0.5V and for the high gain and the FCS based OMA circuits VB1 and VB2 is 0.5V and -0.5V respectively and model parameters of 0.25 μm level 3 CMOS process provided by MOSIS. Also all the gain results are referenced to a resistance of 2.4 KΩ.

The simulation results are presented for one output as the outputs are similar. Fig. 6 shows the input voltage range for all the realizations. It is clear that the input voltage range of the wide range OMA is the higher (about four times of that of the modified OMA). The gain for each realization is displayed in Fig. 7. It can be shown that the FCS – based OMA circuit gives the highest gain and largest bandwidth. On the other hand, the wide range OMA gives the lowest gain but it gives the widest input range. THD [11], noise analysis and other simulation results are summarizes in table (5). Also the gain values obtained from the hand analysis are summarized in table (5).

4. Applications

In the following subsections, several applications of the OMA circuits are presented, and PSPICE simulation results are given to verify the performance of the OMA.

4.1. Current Amplifier

The OMA is a versatile amplification circuit because of the floating output terminals which allows series connection of the feedback to the output, and provides thus the possibility of realizing current input and output configurations. Therefore it may be used to obtain current mode circuits when configured in a way similar to the corresponding voltage mode op-amp circuits as described by the theory of adjoint networks. An illustrating example of the above mentioned theory is the circuit of inverting and non-inverting current amplifier shown in Fig. 8(a, b) respectively. The output currents of these circuits are given by

$$I_o = -I_{IN}\left(1+\frac{R_1}{R_2}\right) \tag{7}$$

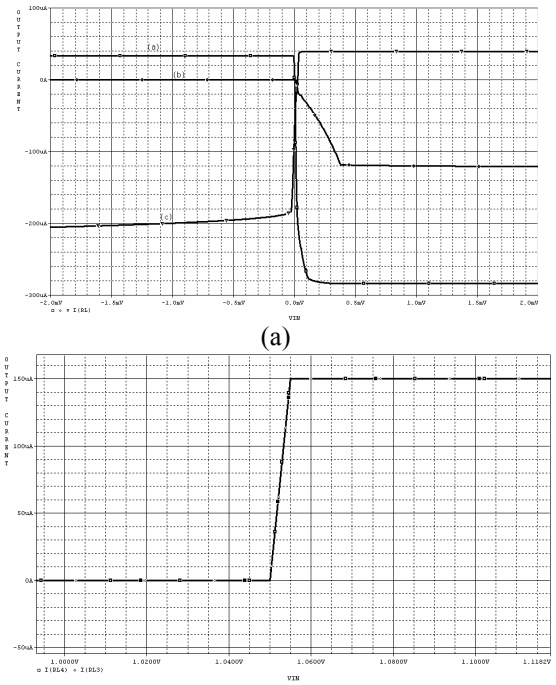

Fig. 6. (a) The output currents of the modified OMA, the wide range OMA and the high gain OMA circuits respectively; (b) The output current of the FCS – Based OMA circuit.

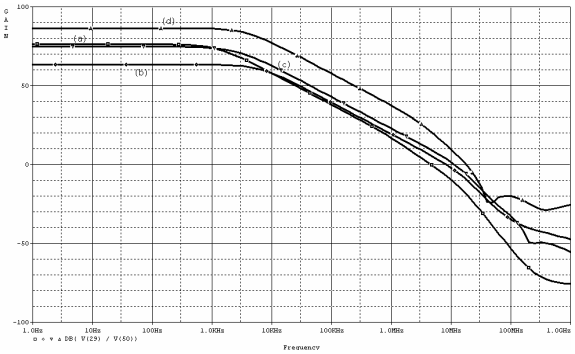

Fig. 7. The gain of the modified OMA, wide range OMA, high gain OMA and the FCS – Based OMA circuits.

$$I_o = I_{IN}\frac{R_1}{R_2} \tag{8}$$

PSPICE simulation of the inverting current amplifier is shown in Fig. 9(a) while the simulation of the non-inverting current amplifier is shown in Fig.9 (b). By observing the simulation results it can

be shown that the OMA can work as a current amplifier with a high accuracy in the output current values. The simulation was made for the inverting and non-inverting current amplifier using the different realizations of the OMA circuits.

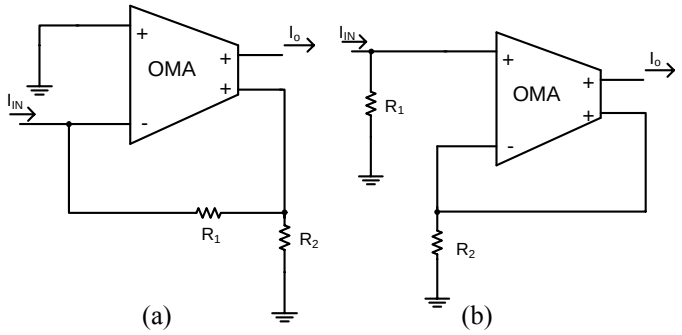

Fig8. (a) Inverting current amplifier using OMA; (b) Non-inverting current amplifier using OMA

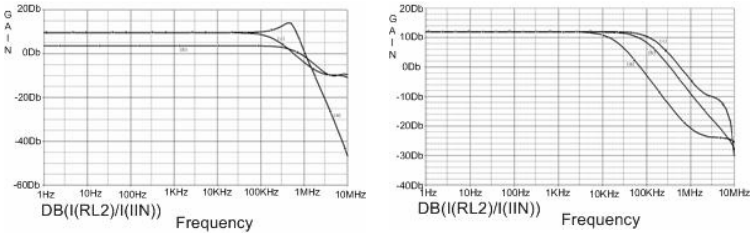

Fig. 9. (a) The inverting current amplifier output using the modified OMA , the wide range OMA and the high gain OMA circuits respectively; (b) The non-inverting current amplifier output using the modified OMA, the wide range OMA and the high gain OMA circuits respectively.

4.2. Voltage Amplifier

The OMA can be used in the voltage mode circuits. A non-inverting voltage amplifier is shown in Fig. 10(a) and the output voltage is given by

$$V_O = V_{IN}\left(1+\frac{R_2}{R_1}\right) \tag{9}$$

This circuit can also be used as a voltage-to-current converter where the output current is taken from the other output of the OMA. The output current from this circuit is given by

$$I_O = \frac{V_{IN}}{R_1} \tag{10}$$

The simulation results for the voltage amplifier and the voltage-to-current converter are shown in Fig. 10(b, c) respectively. The simulation was made using the different realizations of the OMA and the results are the same.

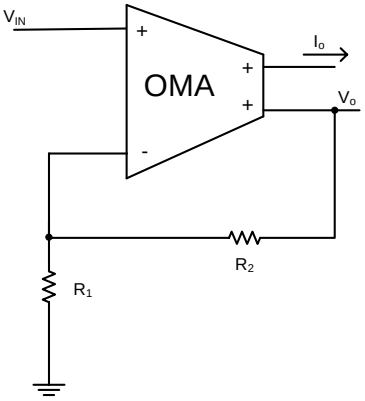

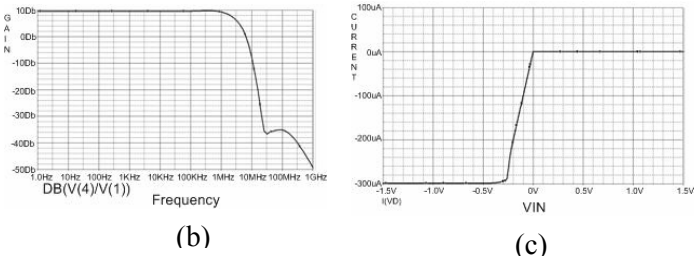

Fig. 10. (a) The voltage amplifier using the OMA; (b) the amplifier output using different OMA realizations;(c) The voltage-to-current converter output for different OMA realizations.

4.3. Sallen-Key Bandpass Filter

Sallen-Key (SK) well-known family of filters [12, 13] requires only one op-amp per biquad. Hence, they are simple and attractive for low power applications. Moreover, since the filters are based on one active element, they are optimum in terms of noise and linearity performance. SK bandpass filter is presented here with minimum number of passive component as shown in Fig. 11(a) is similar to that shown in [12, 13]. This design example is presented here to show that the OMA can be used in many applications like the filtering function presented here.

The transfer function of the filter can be expressed as

$$\frac{V_o}{V_{IN}} = \frac{sK\frac{G_1}{C_1}}{s^2+s\left[\frac{G_1+G_2(1-K)+G_3}{C_1}+\frac{G_3}{C_2}\right]+\frac{G_3}{C_1C_2}(G_1+G_2)} \tag{11}$$

Where

$$K = 1 + \frac{R_4}{R_5} \qquad (12)$$

One design procedure for obtaining a solution for the values of the network elements is to choose an equal – valued resistor and equal – valued capacitors. Thus

$$R_1 = R_2 = R_3 = R \qquad C_1 = C_2 = C \qquad (13)$$

In this case, the natural center frequency (ω_o) and quality factor (Q) are given by

$$\omega_o = \frac{\sqrt{2}}{RC} \qquad (14)$$

$$Q = \frac{\sqrt{2}}{4 - K} \qquad (15)$$

The PSPICE simulation results for the circuit shown in Fig 11(a) is shown in Fig 11 (b) for the filter characteristics, where R_1=R_2=R_3=R = 1.5 kΩ, R_4= 5.7 kΩ, R_5 =2 kΩ and C_1 = C_2 = C = 5nf.

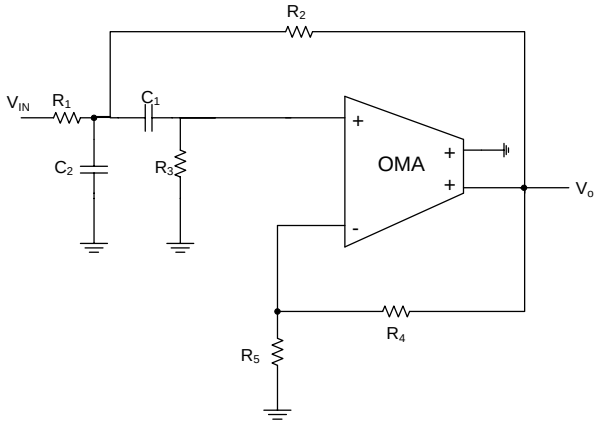

(a)

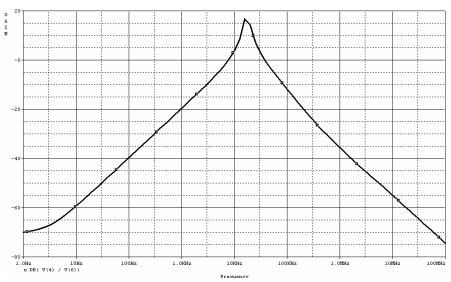

(b)

Fig. 11. (a) Sallen-Key band pass filter using OMA; (b) The filter output using the proposed OMA circuits

4.4 New Proposed OMA – Based Grounded Inductor

Simulated inductors employing active elements [12] are widely used in various applications. A simulated inductor can be realized by using three OMA, one floating capacitor and two floating resistors as shown in Fig. 12(a). The simulated inductance of the simulated inductor is given by

$$L = CR_1R_2 \qquad (16)$$

PSPICE simulation shown in Fig. 12(b) is done to verify that the input impedance of the circuit of Fig. 12(a) behaves as an inductor.

As a design example, a second order low pass and high pass filter is simulated using the proposed inductor. The simulation results of the filter are shown in Fig. 12(c). The filter component values are chosen to a achieve f_o = 63.6 kHz.

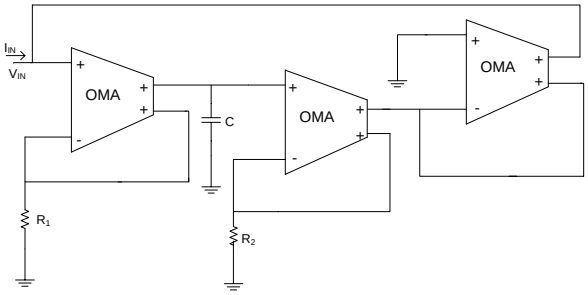

(a)

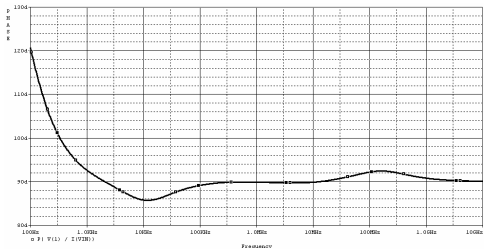

(b)

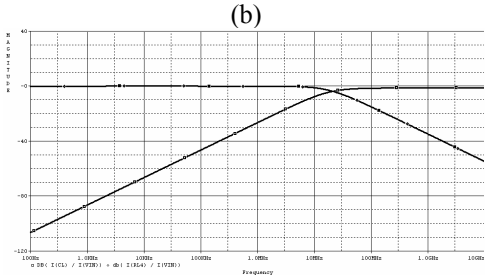

(c)

Fig. 12. (a) The simulated grounded inductor using the OMA; (b) The phase of input impedance of the inductor; (c) Low pass and high pass filter response using the proposed inductor

5. Conclusion

In this paper, many realizations of the OMA were presented. One realization depends on the differential pair, but its input voltage range was small due to the differential pair non-linearity. So the dynamic biasing circuit was used to get another realization with larger input voltage range. The gain of the second configuration was smaller than of the first realization. Then the FCS was used in the OMA realization to get higher gain and this idea gets better results. So a realization which completely depends on the FCS as a building block was introduced and gives better results than the other realizations. Design examples are also presented to show how to use the OMA and its accepted performance with these applications.

References

1. Alzaher, H., Ismail, M.: *A CMOS fully balanced four-terminal floating nullor*. In: IEEE Trans. Circuits Syst. I., Vol. 49(2002), No. 4, 2002, p. 413- 424.
2. Huijsing, J. H.: *Design and application of the operational floating amplifier*. In: Analog Integrated Circuits and Signal Proc., Vol. 4(1992), 1992, p. 115 - 129.
3. Mahmoud, S. A., Soliman, A. M.: *The differential difference operational floating amplifier: A new block for analog signal processing in MOS technology.* In: IEEE Trans. Circuits Syst. II., Vol. 45(1998), No. 1, 1998, p. 148- 158.
4. Awad, I.A., Soliman, A. M.: *A new approach to obtain alternative active building blocks realizations based on their ideal representations*. In: Frequenz, Vol. 54(2000), No. 11-12, November-December 2000, p. 290-299.
5. Laopoulos, T., Siskos, S., Bafleur, M., Givelin, P., Tournier, E.: *Design and application of an easily integrable CMOS operational floating amplifier for the megaHertz range*. In: Analog Integrated Circuits and Signal Proc., Vol. 7(1995), 1995, p. 104 – 111.
6. Razavi, B.: *Design of analog CMOS integrated circuits*. McGraw-Hill, New York, 2001.
7. Yuan, F.: *Low-Voltage CMOS current-mode circuits: topology and characteristics*. In: IEE Proc. Circuits Devices Syst., Vol. 153(2006), No. 3, 2006, p. 219- 230.
8. Mita, R., Palumbo, G., Pennisi, S.: *Low-Voltage high-drive CMOS current feedback op-Amp*. In: IEEE Trans. Circuits Syst. II., Vol. 52(2005), No. 6, 2005,p. 317- 321.
9. Youssef, M. A., Soliman, A. M.: *A new CMOS rail – to – rail low distortion balanced output transconductor.* In: Analog Integrated Circuits and Signal Proc., Vol. 40(2003), 2003, p. 75-82.
10. Bruun E, E.: *CMOS current conveyors*. In: IEEE International Symposium on Circuits and Systems, Circuits and Systems Tutorial, 1994, p. 632-641.
11. Giustolisi, G., Palumbo, G.: *Techniques for evaluating harmonic distortion in class-AB output stages: a tutorial*. In: Analog Integrated Circuits and Signal Proc., Vol. 47(2006), 2006, p. 323-334.
12. Huelsman, L. P.: *Active and Passive Analog Filter Design: an Introduction*. McGraw-Hill, Singapore, 1993.
13. Chen, W.: *Passive and Active Filters Theory and implementations*. John Wiley & Sons, Singapore, 1986.

Table 5. A summary of the simulation results

	Modified OMA circuit	Wide range OMA	High gain OMA	the FCS – Based OMA circuit
Circuit Fig.	2	3	4	5
# of transistor	32	37	30	21
Input range mV	0 to 0.117	0 to 0.38	-0.02 to 0.04	1050 to 1055
3-dB bandwidth kHz	1.2	6.6	2.7	6.6
Unity gain frequency MHz	4.6	8.145	11.2	20
Gain Db(simulated)	76.2	63.4	74.7	86.4
Gain Db(calculated)	74.3	64.7	77.4	88.4
Power dissipation mW	0.911	1.47	2.6	0.151
THD for a sinusoid of 1kHz	42.6%	42.6%	37.7%	42%
Noise level $nv/\sqrt{Hz}$	5.4	0.473	0.838	18.84